LIQUID CRYSTALS, 1993, VOL. 14, NO. 2, 453–461

Electromechanical effect in an antiferroelectric liquid crystal

by N. ÉBER* and L. BATA

Research Institute for Solid State Physics, Hungarian Academy of Sciences,
H-1525 Budapest, P.O. Box 49, Hungary

The electromechanical properties of a compound exhibiting an antiferroelectric phase were investigated. An electric field induced antiferroelectric–ferroelectric transition could be detected by vibration analysis. In the antiferroelectric state the vibrations almost vanish while in the ferroelectric state the electromechanical effect has the same magnitude as in the chiral smectic C* phase.

1. Introduction

In the past decade a considerable attention was paid to the investigation of ferroelectric liquid crystals owing to the electrooptical effects which can be utilized in various applications [1, 2]. These electrooptical effects are based on the electric field induced reorientation of the optical axis of a planar S_C^* liquid crystal cell.

The reorientation of the director is accompanied by electric field induced mechanical vibrations [3]. This electromechanical effect is typically linear in the ferroelectric phase and quadratic in the other phases. The characteristics of these vibrations were investigated in various cell geometries and on several substances [4–11]. It was proved [10, 11] that vibrations exist in three orthogonal directions, parallel as well as normal to the cell plates and the smectic layers, though the mechanisms leading to these vibrations are thought to be different [11].

It was shown recently that some chiral smectic liquid crystals exhibit tristable switching [12] instead of the bistable one characteristic of the ferroelectric S_C^* phase. This behaviour was explained as due to a new phase ($S_{C_A}^*$) possessing antiferroelectric structure [13]. The transition from the antiferroelectric to the ferroelectric state can be induced by either increasing the temperature or applying a high enough electric field [14].

The aim of our investigation was to determine how this phase transition influences the electromechanical effect of a compound exhibiting an antiferroelectric phase.

2. Experimental

Measurements were carried out on the mixture CS-4000 (Chisso) which exhibits an antiferroelectric phase ($S_{C_A}^*$) in a wide temperature interval including the room temperature. The complete phase sequence of the substance is the following:

$$C \xrightarrow{-10^\circ C} S_{C_A}^* \xrightarrow{82^\circ C} S_C^* \xrightarrow{84^\circ C} S_A^* \xrightarrow{100^\circ C} I.$$

The experimental set-up was similar to the one used in previous measurements [3, 4]. One plate of a 20 μm thick sandwich cell was connected to the membrane of a loudspeaker allowing almost free motion of this plate with respect to the fixed one in a direction parallel to the plates (Y axis) while limiting motions in the other directions. Three piezoelectric accelerometers (Brüel–Kjær 4375) were mounted on the moving

* Author for correspondence.

0267–8292/93 $10·00

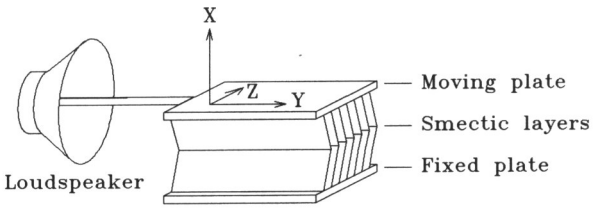

Figure 1. Simplified experimental geometry. The moving plate is connected to the membrane of the loudspeaker. Arrows indicate the sensitive directions of the accelerometers. X, perpendicular to the plates; Y, parallel to the membrane axis (and the smectic layers); and Z, parallel to the plates, normal to the membrane axis.

plate in orthogonal directions detecting the vibrations perpendicular to the plates (X axis), parallel to both the plates and the membrane axis (Y axis) and parallel to the plates but perpendicular to the membrane axis (Z axis) respectively. The orientation of these vibration directions with respect to the cell geometry is shown in figure 1.

The acceleration signal was analysed by a lock-in amplifier which could be tuned either to the excitation frequency or to its double. This allowed us to choose between the basic harmonic (linear effect) and the second harmonic (quadratic effect) component of the acceleration.

In order to obtain planar orientation we used polyimide surfaces rubbed in the Z direction. Surface orientation was aided by shearing the cell with the loudspeaker along Y at the S_A^*–I phase transition. The orientation was then improved by applying an AC electric field to the cell at the higher temperature end of the antiferroelectric phase. Finally, a fairly homogeneous planar texture was obtained with the smectic layers aligned parallel to the Y axis.

3. Results

The electromechanical vibrations were analysed as a function of temperature, applied voltage and vibration direction. The frequency of the applied voltage was chosen to $f = 5\,\text{kHz}$, this produced easily measurable vibration amplitudes.

First, we focus our attention on the vibrations parallel to both the electrodes and the smectic layers (Y direction). These vibrations are thought to be the result of a backflow phenomenon accompanying the reorientation of the director.

Figure 2 (*a*) shows the temperature dependence of the linear component of the acceleration. It is seen that though vibrations could be detected in the S_A^* and S_C^* as well as in the $S_{C_A}^*$ phase, the linear effect is pronounced around the S_C^* phase only. Increasing the temperature above the S_C^*–S_A^* phase transition the acceleration decreases gradually. Decreasing the temperature below the S_C^*–$S_{C_A}^*$ phase transition the acceleration remains large until a critical temperature is reached where the amplitudes drop sharply.

The temperature dependence of the quadratic component of the acceleration (see figure 2 (*b*)) is slightly different. The quadratic effect is largest at high temperatures in the S_A^* phase, then it has a minimum near the S_C^*–S_A^* phase transition. In the S_C^* and in the high temperature end of the $S_{C_A}^*$ phase the amplitudes are still high, however, they decrease sharply at the same critical temperature as the linear ones. This critical temperature depends on the applied voltage.

The vibration amplitudes should increase with increasing applied voltage. Linear and parabolic curves are expected for the basic and the second harmonic components of the acceleration [6, 7]. Figures 3 (*a*)–(*b*) show that this holds in the low voltage region

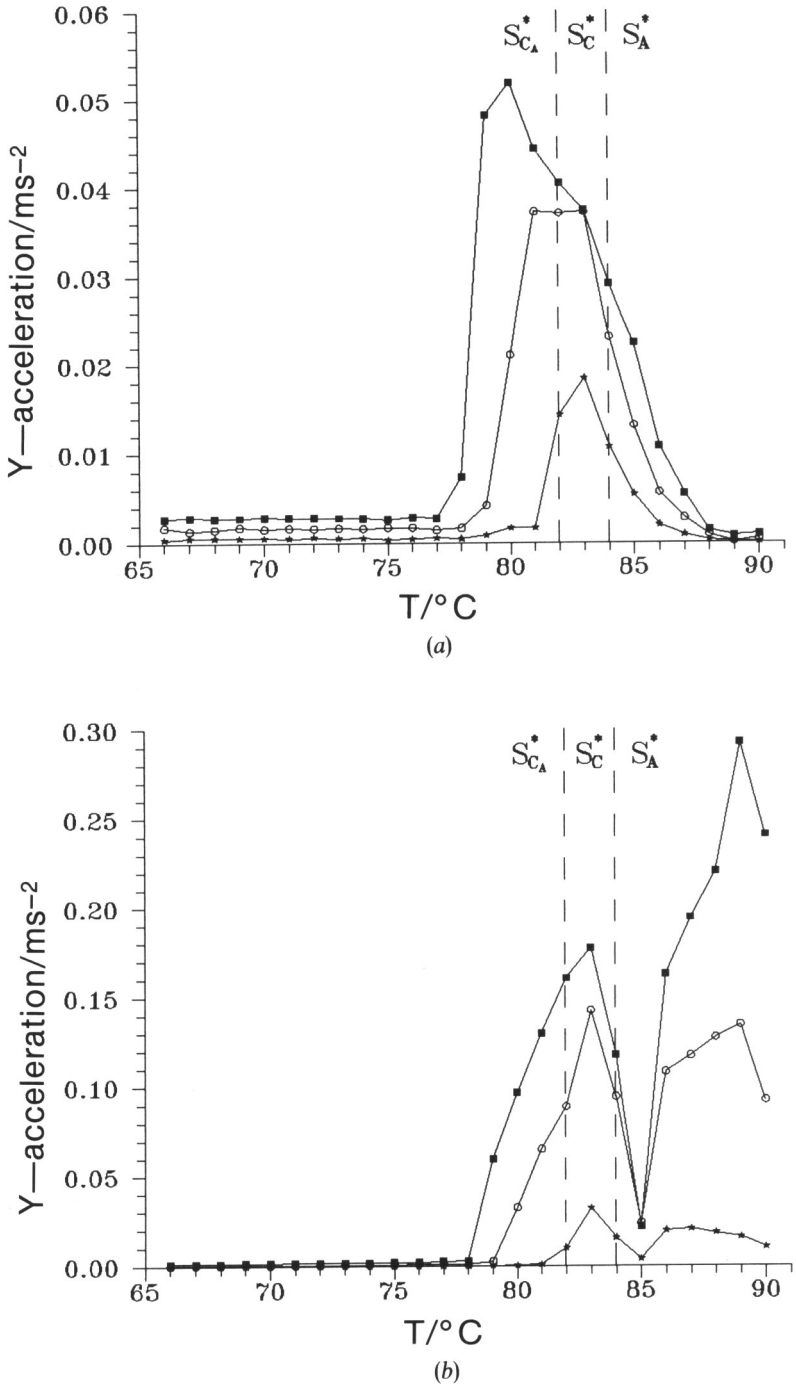

Figure 2. Temperature dependence of the acceleration along *Y*. The excitation frequency is $f = 5$ kHz. (*a*) Basic harmonic (linear) component of the acceleration, ∗, 10 V; ○, 30 V; and ■, 50 V. (*b*) Second harmonic (quadratic) component of the acceleration ∗, 10 V; ○, 30 V; and ■, 50 V.

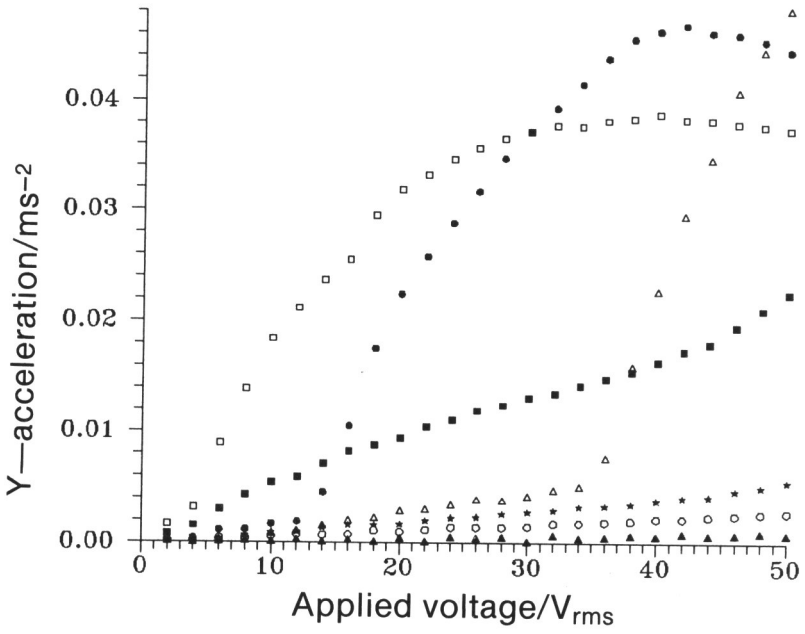

(*a*)

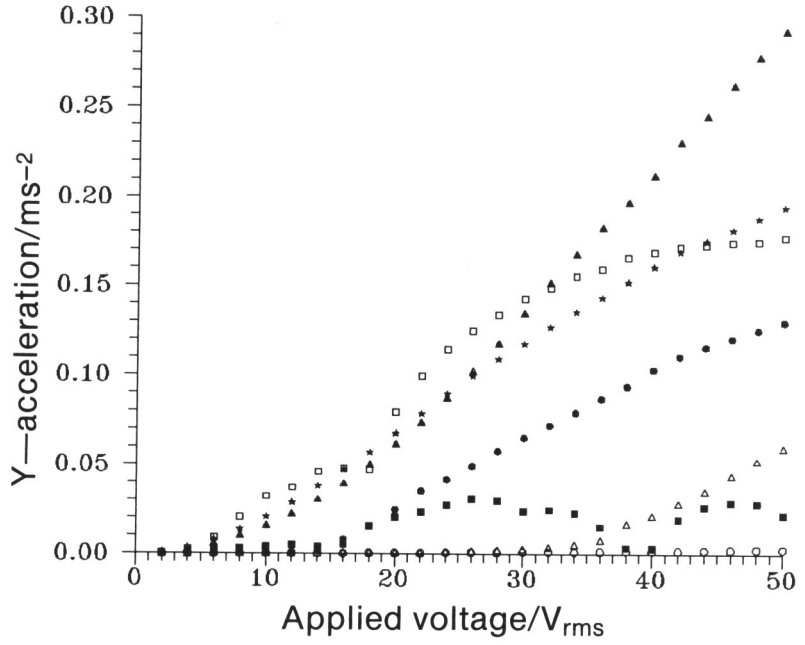

(*b*)

Figure 3. Voltage dependence of the acceleration along *Y*. The excitation frequency is $f = 5$ kHz in the S_A^* phase at 89°C (▲), 87°C (∗), 85°C (■), the S_C^* phase at 83°C (□) and the $S_{C_A}^*$ phase at 81°C (●), 79°C (△) and 77°C (○). (*a*) Basic harmonic (linear) component of the acceleration. (*b*) Second harmonic (quadratic) component of the acceleration.

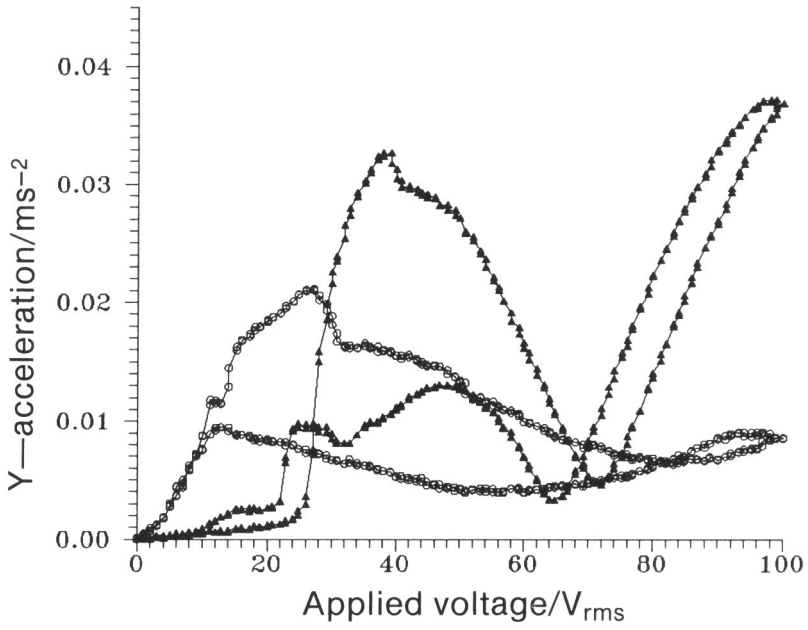

(*a*)

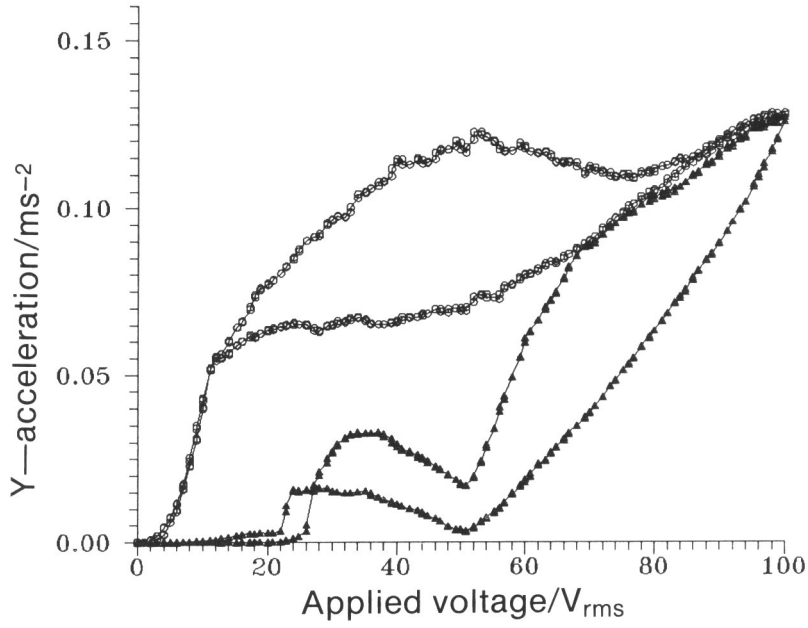

(*b*)

Figure 4. Hysteresis in the voltage dependence of the acceleration along *Y*. The excitation frequency is $f = 5$ kHz in the S_C^* phase at 83·2°C (○) and the $S_{C_A}^*$ phase at 78·1°C (▲). (*a*) Basic harmonic (linear) component of the acceleration. (*b*) Second harmonic (quadratic) component of the acceleration.

in the S_A^* and the S_C^* phase. The distortion of the curves at higher voltages are due to the fact that the rotation angle of the director becomes large in the full switching regime and it results in a crucial change of the effective material parameters governing the electromechanical effect.

The voltage dependence of the acceleration is quite different in the $S_{C_A}^*$ phase. The vibrations are very weak and follow the expected behaviour below a temperature dependent threshold voltage, but above this threshold the amplitudes increase sharply as in the S_C^* phase. Simultaneous observation of the electrooptical response of the cell have shown that there is hardly any modulation of the transmitted light intensity of the cell at low voltages while above the threshold voltage a S_C^*-like full switching occurs.

The results presented above indicate that in the $S_{C_A}^*$ phase there exist two distinct regimes. One of them corresponds to the really antiferroelectric state where the electric field cannot induce a large deformation of the structure and consequently the amplitudes of the mechanical vibrations are very small. The other one should be a ferroelectric state characterized by full electrooptical switching and large amplitude vibrations. These two regimes are sharply separated in the temperature applied voltage space.

Figures 4 (*a*)–(*b*) demonstrate that the voltage dependence of the acceleration may exhibit a hysteresis. In the S_C^* phase this hysteresis is probably in connection with texture changes (for example layer deformations) occurring besides the full switching. In the $S_{C_A}^*$ phase the hysteresis indicates that the threshold voltages for the antiferroelectric–ferroelectric and the ferroelectric–antiferroelectric transitions are different.

The temperature dependence of these threshold voltages is plotted in figure 5. The thresholds obtained from the linear and quadratic electromechanical responses did

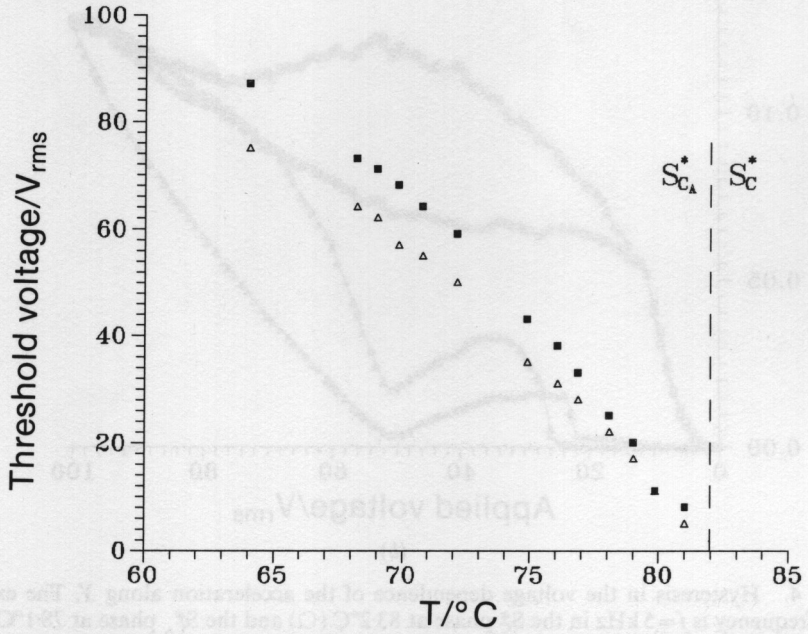

Figure 5. Temperature dependence of the threshold voltages of the transitions from the antiferroelectric to the ferroelectric state (■) and vice versa (△). The excitation frequency is $f = 5$ kHz.

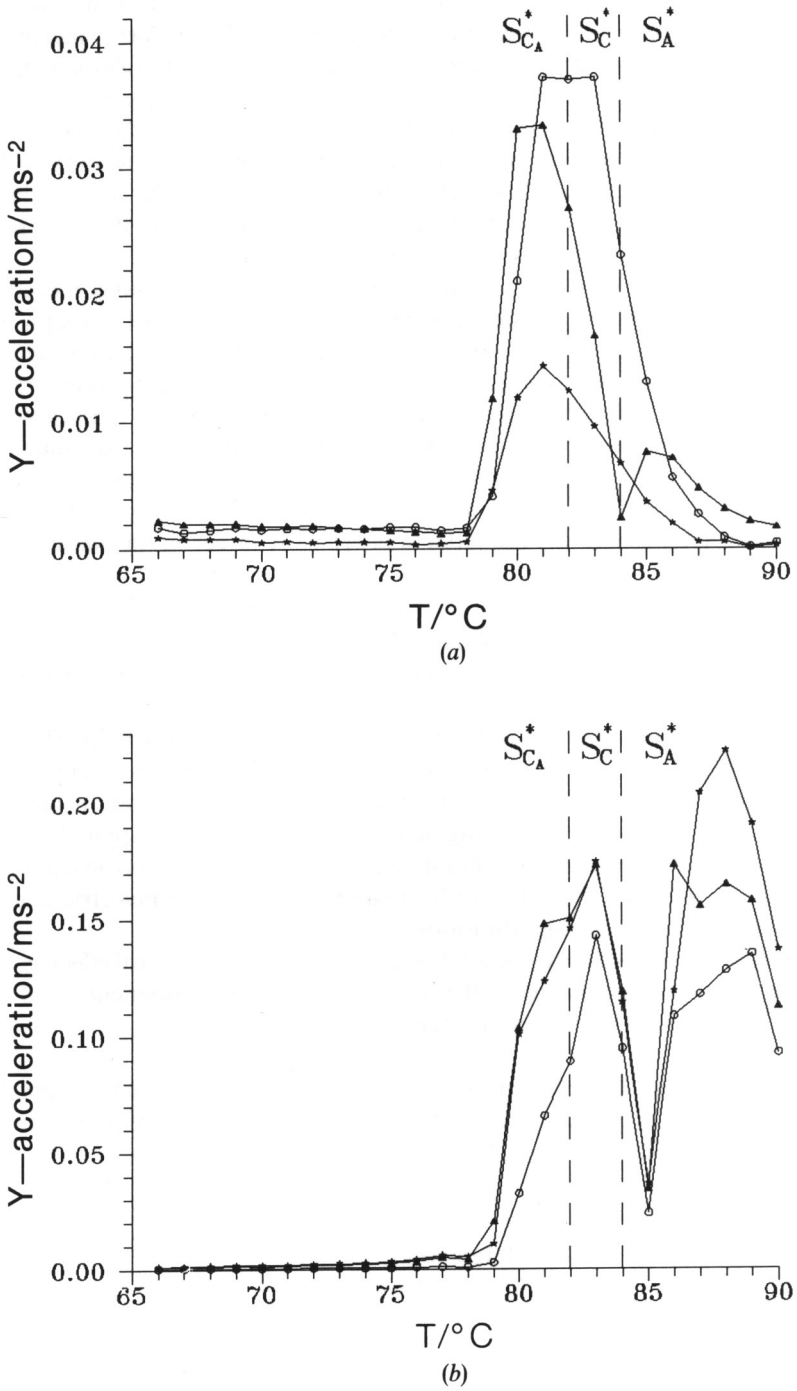

Figure 6. Temperature dependence of the accelerations along the X axis (∗), the Y axis (○) and the Z axis (▲). The excitation frequency is $f=5$ kHz. (*a*) Basic harmonic (linear) components of the accelerations. (*b*) Second harmonic (quadratic) components of the accelerations.

coincide. The threshold for the antiferroelectric–ferroelectric transition was always higher than for the opposite transition, and both thresholds were increasing monotonically towards lower temperatures. We could not induce a transition into the ferroelectric stage below 62°C due to the output voltage limit of our generator.

The electric field induced mechanical vibrations are not limited to the direction of the Y axis (i.e. against the loudspeaker membrane), they have components in the other two orthogonal directions (X and Z) as well, moreover, they are of the same order of magnitude. This is illustrated in figures 6 (*a*)–(*b*). Other characteristics of these (along X or Z) vibrations are very similar to those presented in figures 3–5.

Throughout this paper we characterized the vibrations by the directly measured quantity, the acceleration (a) of the moving plate. One can easily obtain the displacement (d) of the plate using the expressions $a = d\omega^2$ for the linear and $a = d(2\omega)^2$ for the quadratic electromechanical effect, i.e. the displacements are proportional to the acceleration ($\omega^2 \approx 10^9\ s^{-2}$). The maximum displacements corresponding to the accelerations plotted in figures (2–6) are approximately 0·05 nm for the basic harmonic and 0·075 nm for the second harmonic component. This shows that the linear and the quadratic electromechanical effects were of the same order of magnitude in the investigated compound, moreover, the latter was typically larger in all phases.

4. Conclusion

Electric field induced mechanical vibrations could be detected in the S_A^*, S_C^* and $S_{C_A}^*$ phases. The vibrations were a superposition of linear and quadratic (second harmonic) contributions. Two distinct regimes could be distinguished in the electromechanical response of the $S_{C_A}^*$ phase. These two regimes correspond to an antiferroelectric and a ferroelectric state respectively which are sharply separated. The transition between these states can be induced either by changing the temperature or the applied voltage and can be traced by vibration analysis. The magnitude of the linear electromechanical effect is high in the ferroelectric states only, while the true antiferroelectric state is characterized by almost vanishing vibrations.

A detailed study of the frequency dependence of the electromechanical effect as well as the simultaneous measurement of the various vibration components and the electrooptical response of the cell are in preparation.

We would like to thank Professor Inukai and the Chisso Corporation for supplying us with the liquid crystal substance. This work was supported by the National Scientific Research Fund (OTKA-2946).

References

[1] Clark, N. A., and Lagerwall, S. T., 1980, *Appl. Phys. Lett.*, **36,** 899.
[2] Lagerwall, S. T., Otterholm, B., and Skarp, K., 1987, *Molec. Crystals liq. Crystals*, **152,** 503.
[3] Jákli, A., Bata, L., Buka, Á., Éber, N., and Jánossy, I., 1985, *J. Phys. Lett., Paris*, **46,** L-759.
[4] Jákli, A., Bata, L., Buka, Á., and Éber, N., 1986, *Ferroelectrics*, **69,** 153.
[5] Jákli, A., Éber, N., and Bata, L., 1988, *Liq. Crystals*, **5,** 1121.
[6] Jákli, A., and Bata, L., 1990, *Liq. Crystals*, **7,** 105.
[7] Jákli, A., and Bata, L., 1990, *Ferroelectrics*, **103,** 35.
[8] Éber, N., Bata, L., Scherowsky, G., and Schliwa, A., 1991, *Ferroelectrics*, **122,** 139.
[9] Jákli, A., and Saupe, A., 1991, *Liq. Crystals*, **9,** 519.

[10] ÉBER, N., KOMITOV, L., LAGERWALL, S. T., MATUSZCZYK, M., SKARP, K., and STEBLER, B., 1992, *Ferroelectrics*, **129,** 19.
[11] JÁKLI, A., and SAUPE, A., 1991, *Third International Conference on Ferroelectric Liquid Crystals*, Boulder, Colorado (to be published).
[12] CHANDANI, A. D. L., HAGIWARA, T., SUZUKI, Y., OUCHI, Y., TAKEZOE, H., and Fukuda, A., 1988, *Jap. J. appl. Phys.*, **27,** L729.
[13] CHANDANI, A. D. L., GORECKA, E., OUCHI, Y., TAKEZOE, H., and FUKUDA, A., 1989, *Jap. J. appl. Phys.*, **28,** L1265.
[14] HIRAOKA, K., CHANDANI, A. D. L., GORECKA, E., OUCHI, Y., TAKEZOE, H., and FUKUDA, A., 1990, *Jap. J. appl. Phys.*, **29,** L1473.